Interactions of Acetylene-Derived Thioester Collectors with Gold Surfaces: A First-Principles Study

Xianyang Qiu , Yuechao Qi * , Dezhou Wei , Faming Zhang , Chenghang Wang

Posted Date: 22 January 2024

doi: 10.20944/preprints202401.1544.v1

Keywords: flotation; gold; surface adsorption; DFT; acetylene; collectors

Article

Interactions of Acetylene-Derived Thioester Collectors with Gold Surfaces: A First-Principles Study

Xianyang Qiu [1,2,3],Yuechao Qi [1],Dezhou Wei [1],Zhangfaming [2,3],Chenghang Wang [2,3]

[1] Northeastern University, Shenyang 110819, Liaoning, China;
[2] Institute of Resource Utilization and Rare Earth Development, Guangdong Academy of Sciences, Guangzhou 510651, Guangdong, China;
[3] State Key Laboratory of Separation and Comprehensive Utilization of Rare Metal, Guangzhou 510651, Guangdong, China)
* Correspondence: e-mail@e-mail.com; Tel.: (optional; include country code; if there are multiple corresponding authors, add author initials)

Abstract: The high reactivity of acetylene group the formation of strong chemical bonds with active sites on mineral surfaces, thereby improving the flotation performance of gold minerals. This study utilized Density Functional Theory (DFT) to analyse the quantum chemical parameters of structure, Mulliken population, and the frontier orbitals of a thioester collector containing an acetylene group, PDEC (prop-2-yn-1-yl diethylcarbamodithioate). PDEC is compared with analogous thioester collectors Z-200 and Al-DECDT, and the interaction mechanism of PDEC on the Au(1 1 1) surface is simulated, followed by empirical validation through adsorption experiments. The findings indicate that S atom of PDEC in the carbon-sulfur group exhibit shorter covalent bond lengths, and reduced carbon-sulfur double bonds and Mulliken population, resulting in enhanced electron localization. This confers greater selectivity to PDEC during its adsorption on mineral surfaces. Frontier orbital analysis shows that the electrons of acetylene group possess a notable electron-accepting capacity, significantly influencing frontier orbital energy of PDEC and playing a pivotal role in the bonding interaction with mineral surfaces. Both the S atom in carbon-sulfur group and its acetylene group establish stable adsorption structures with the A(111) surface in a single coordination mode. The adsorption energy sequence is PDEC > Al-DECDT > Z-200. Partial density of states demonstrates that S 3p orbit of carbon-sulfur group hybridize with Au 5d orbit, while the C 2p orbit of the acetylene group engage in weaker back-donation bonding with Au 5d orbit. This is corroborated by electron density difference and post-adsorption Mulliken population analyses, revealing that S atom of carbon-sulfur group in PDEC donate electrons to Au atom, forming dominant positive coordination bonds, whereas the acetylene group accepts partial electrons from Au atom, resulting in weaker back-donation bonds. The adsorption experiments align with the DFT adsorption energy results.

Keywords: flotation; gold; surface adsorption; DFT; acetylene; collectors

1. Introduction

Gold predominantly exists in its elemental state, typically found in quartz veins, sulfide mineral deposits, and placer deposits [1]. Its economic value and significant role in industrial and technological sectors are well-recognized [2]. Thorough research into gold extraction and purification techniques not only enhances resource utilization efficiency but also fosters sustainable development in related industries [3]. The primary methods for gold beneficiation include gravity separation, flotation, cyanidation, and pyrometallurgy. Gravity separation is effective for coarse-grain gold ores, while flotation suits fine-grain gold ores. Cyanidation, a chemical extraction method, dissolves gold in cyanide solutions, and pyrometallurgy involves processes such as smelting and electrolysis [4,5].

Flotation, a highly efficient method for gold enrichment and recovery, depends critically on the choice and application of collectors [6,7]. Recent decades have seen notable advancements in research on gold flotation collectors, including sulfide collectors, amino acid collectors, and multifunctional

 doi:10.20944/preprints202401.1544.v1

composite collectors, all demonstrating superior efficacy in enhancing gold recovery and selectivity [8–10]. Liu et al.[11] investigated Diisobutyl Monothiophosphate as a collector in gold-pyrite flotation, achieving enhanced gold recovery while effectively suppressing pyrite. Oluwabunmi et al.[12] utilized P-Xanthate and amino glycol as collectors, significantly boosting gold recovery in environments with a pH of 9.2. Tan et al.[13] developed a novel collector, ZL4020, outperforming butyl xanthate in increasing gold recovery at the Da Hong Shan gold mine. Beattie et al.[14] employed X-ray Photoelectron Spectroscopy (XPS) to examine the chemisorbed geometries of MBT and DTP collectors on gold and gold-silver alloy surfaces, yielding profound insights into gold surface reactions. Acetylene-based collectors have garnered interest for their high reactivity, enabling strong chemical bonding with sulfides or other reactive sites on mineral surfaces, thereby enhancing mineral flotation performance, particularly in complex ore separation [15]. It was hypothesized that the acetylene group's hydrogen may interact with metals like Cu, Au, and Ag in aqueous solutions, forming organometallic compounds [16]. Burdonov et al.[17] explored a novel collector, 2-methyl-3-butyn-2-ol, showing promise in augmenting gold recovery from challenging-to-float sulfide minerals through electrostatic adsorption on pyrite surfaces. Yushina, T. I.[18] applied the Molecular Mechanics (MM2) method to assess the selective fixation of acetylene-containing alcohol collectors, suggesting potential additional gold recovery rates of 2.4% to 5.0% from gold-bearing ores.

Recently, the increasing application of Density Functional Theory (DFT) in flotation research has offered fresh insights into the electronic structure of minerals and their flotation behavior. Liu et al.[19] employed DFT to elucidate the molecular interaction mechanism of Diisobutyl Monothiophosphate as a collector in gold pyrite flotation. It revealed that this collector effectively binds to gold mineral surfaces, enhancing gold recovery rates. Yushina et al.[18] investigated the electronic interaction mechanism of unsaturated tertiary alcohol collectors in gold sulphide ore flotation via DFT simulations. Results indicated that these collectors significantly enhance gold flotation selectivity.In conclusion, employing DFT in gold flotation research offers novel insights into the electronic structure of gold minerals and their flotation dynamics. DFT simulations enable researchers to delve into the interaction mechanisms between collectors [20] and gold mineral surfaces, facilitating the design of more efficient and selective flotation collectors [21].

The motivation of this work is to unveil the mechanism of a thioester collector with an acetylene group, PDEC (prop-2-yn-1-yl diethylcarbamodithioate), on the Au(1 1 1) [22]surface using Density Functional Theory (DFT) calculations [23].To further this investigation, the Highest Occupied Molecular Orbital (HOMO), Lowest Unoccupied Molecular Orbital (LUMO)[23], and Fukui function [24] were applied to distinguish and highlight the unique attributes and superiorities of PDEC over other non-ionic thioester collectors. Moreover, the reaction mechanism was meticulously analyzed through the adsorption energy of the collector molecules on the Au surface, the Partial Density of States (PDOS)[25,26], and the difference density. Subsequently, Adsorption experiments on gold powder were performed to corroborate the DFT adsorption energy findings. This study contributes novel perspectives on the adsorption mechanisms of acetylene-based collectors on Au surfaces and is instrumental in guiding the development of innovative collectors for gold.

2. Methods

2.1. Model and Parameters

The crystal and surface models of gold (Au), along with the molecular and adsorption models of the collectors, were developed using Visualizer and Amorphous cells tools in Materials Studio 2018. First-principles calculations utilized the CASTEP and Dmol^3 modules [27]. CASTEP was employed for model optimization, adsorption energy calculations, Partial Density of States (PDOS), and Electron Density Difference. Conversely, Dmol^3 was used for frontier orbital analysis and Fukui function assessments. Ultrasoft pseudopotentials facilitated the modeling of interactions between ionic valence and valence electrons.

The Au(1 1 1) surface holds a significant role in surface science and nanotechnology, attributed to its distinctive chemical and physical attributes [28]. As shown in Figure 1,following the

 doi:10.20944/preprints202401.1544.v1

optimization of the Au crystal cell, an Au(1 1 1) surface consisting of eight atomic layers was developed. This optimization entailed stabilizing the bottom two layers and permitting the relaxation of the top six atomic layers. Furthermore, a 15Å vacuum layer was established above the surface.

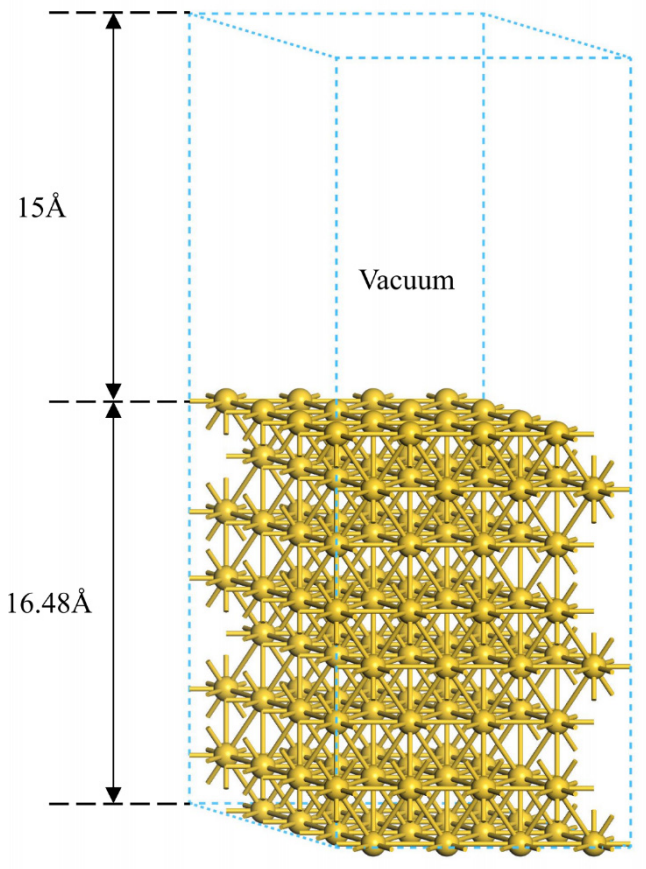

Figure 1. Used Au slab in the CASTEP calculations (where golden yellow spheres represent Au atoms, respectively).

After evaluating each exchange-correlation function's truncation energy, GGA_PBESOL demonstrated the closest convergence value to the experimental data, with an error margin of only 1.20%, which falls within the acceptable range. Consequently, GGA_PBE was selected as the exchange-correlation function. The chosen truncation energy was set at 380 eV, and a k-point grid of 2 × 2 × 1 was applied for all three surface configurations. Structural optimization was performed using the BFGS algorithm [29], adhering to specific convergence criteria: 0.05 eV/Å for interatomic interaction forces, 0.1 GPa for internal stress, 2×10^{-3} Å for maximum atomic displacement, and 2×10^{-6} eV/atom for self-consistent field accuracy [30].

Two types of thioester collectors, Z-200 (O-isopropyl ethylcarbamothioate) and Al-DECDT (allyl diethylcarbamodithioate) , were used as a comparison with PDEC (prop-2-yn-1-yl diethylcarbamodithioate), the molecular structure optimization of PDEC, Z-200, Al-DECDT utilized the same parameters, as illustrated in Figure 2. For Dmol^3 calculations, the Gamma point was employed for k-points, ensuring consistency with the parameters used in CASTEP.

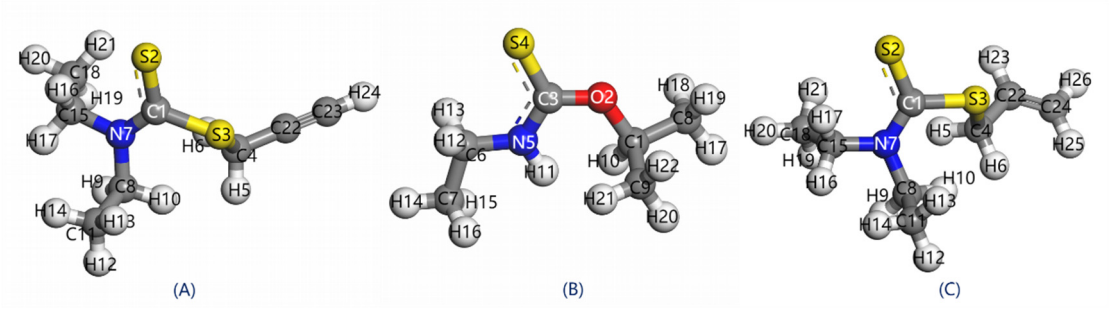

Figure 2. Optimized structures of the investigated (A) PDEC, (B) Z-200, (C) Al-DECDT(where yellow, gray, blue, red, white spheres represent S, C, N, O, H atoms, respectively).

2.2. Adsorption Energy Calculation

The calculation of the collector's adsorption energy on the Au surface employs the formula below. E_{ad} signifies the adsorption energy, $E_{(Au\text{-}surface+\alpha)}$ the system's total energy post-adsorption, $E_{Au\text{-}surface}$ the energy of the Au crystal face, and E_{α} the energy of the collector. A negative value of E_{ad} suggests spontaneous adsorption, with a larger absolute value indicating greater ease of adsorption.

$$E_{ad}=E_{(Au\text{-}surface+\alpha)}-E_{Au\text{-}surface}-E_{\alpha} \quad (1)$$

2.3. Adsorption Experiments

For the adsorption experiments, the UV-Visible Spectrophotometer (UV2600, Shunyu Hengping Scientific Instrument Co., Ltd., Shanghai, China) was utilized to quantify the collector adsorption on gold powder surfaces. Each experiment involved adding 2g of gold powder (Au ＞99.99%, particle size -0.074mm, sourced from Zhongnuo New Material Technology Co., Ltd., Beijing, China) to a collector solution of specified concentration, The solution's pH was adjusted to 8.8 using sodium hydroxide, followed by 30 minutes of magnetic stirring. Post-reaction, the mixture underwent centrifugation by TG16-WS machine (Xiangyi Group, Changsha, China) at 9000 r/min for 15 minutes. The UV absorbance of the resulting filtrate was measured to ascertain the adsorption quantity of collector on the gold powder, determined by the molar difference of the collector before and after adsorption.

3. Results and Discussion

3.1. Structure and Mullinken Population

In the CASTEP module of Materials Studio 2018, Collectors and analyzed key bond lengths, compound layouts, and atomic charge distributions was optimized, as detailed in Table 1. The S atom in the carbon-sulfur group of the collectors exhibit covalent bond lengths in the order of PDEC > Al-DECDT > Z-200. Shorter bond lengths denote stronger electron localization, indicating a lower propensity for electron loss in S atom of Z-200 and Al-DECDT compared to PDEC. Conversely, the population of the carbon-sulfur double bond in the collectors is ordered as PDEC < Al-DECDT < Z-200, with higher population numbers reflecting stronger covalent bonding. This suggests weaker electron localization in S atom of Z-200 relative to PDEC and Al-DECDT, aligning with the bond length findings. Consequently, PDEC exhibits superior selectivity in mineral collection over Al-DECDT and Z-200, based on the carbon-sulfur double bond population. Furthermore, the absolute charge values on the sulfur atoms in the reaction center's carbon-sulfur group of each collector are ranked as Z-200 > Al-DECDT > PDEC. Higher absolute charge values correlate with intensified electrostatic interactions with metal ions on the mineral surface. However, due to the non-directional nature of electrostatic interactions, stronger interactions do not necessarily enhance collector selectivity. Thus, in terms of sulfur atom charge, the selectivity ranking of the collectors is PDEC > Al-DECDT > Z-200.

 doi:10.20944/preprints202401.1544.v1

Table 1. The magnitude of bond length and the Mullinken population of collectors.

Collectors	Bond length (Å)	Mullinken population of bond	Mullinken population of atom charge				
PDEC	C1-S2	C1-S2	S2	C1	N7	S3	C23
	1.669	0.90	-0.14	-0.17	-0.27	0.23	-0.38
Z-200	C3-S4	C3-S4	S4	C3	N5	O2	
	1.651	0.94	-0.19	0.22	-0.55	-0.41	
Al-DECDT	C1-S2	C1-S2	S2	C1	N7	S3	C24
	1.664	0.90	-0.15	-0.17	-0.26	0.18	-0.62

3.2. Frontier Orbital Analysis

Energy calculations for the optimized models of various collectors were conducted using the Dmol^3 module, with the resulting frontier orbital energies detailed in Table 2. In the context of substrates engaged in complex nucleophilic or electrophilic reactions, the proximity of energy of LUMO+1 to LUMO necessitates an examination of LUMO+1[31]. Figure 3 illustrates the significant contribution of the acetylene group to the frontier orbital energies of PDEC, particularly to LUMO+1. This underscores the crucial role of acetylene group in facilitating bond formation between PDEC and the mineral surface. The delocalized nature of the electrons of acetylene group enables them to accept additional electrons from themetal atoms of mineral, thereby forming more stable feedback bonds.

Table 2. Frontline orbital energy of collectors.

Collectors	Frontline orbital energy (eV)		
	HOMO	LUMO	LUMO+1
PDEC	-4.708	-2.077	-0.608
Z-200	-4.515	-0.812	0.510
Al-DECDT	-4.456	-1.942	-0.895

 doi:10.20944/preprints202401.1544.v1

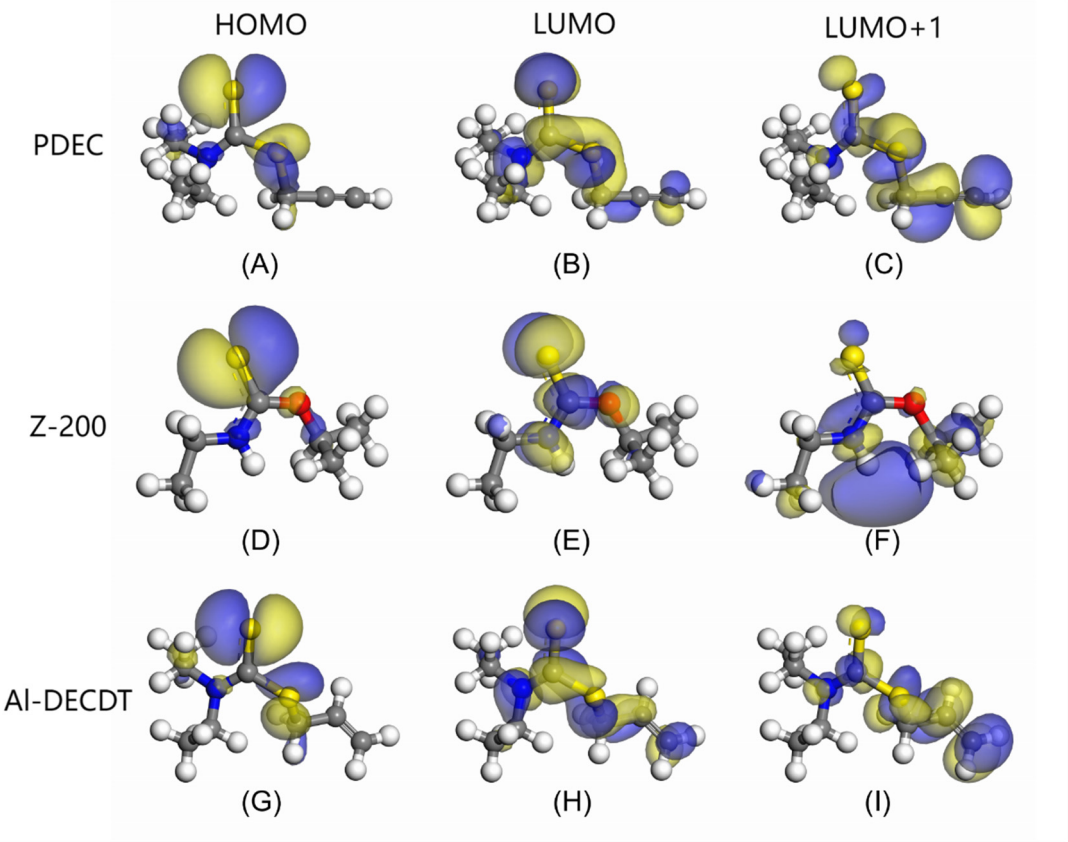

Figure 3. HOMO of the (A) PDEC,(D) Z-200 and (G) Al-DECDT clusters, LUMO of the (B) PDEC,(E) Z-200 and (H) Al-DECDT clusters, LUMO+1 of the (C) PDEC,(F) Z-200 and (I) Al-DECDT clusters (where yellow, gray, blue, red, white spheres represent S, C, N, O, H atoms, respectively).

Fukui functions f_{w+} and f_{w-}, quantify the propensity for nucleophilic and electrophilic reactions at specific atoms or groups within a molecule. Table 3 demonstrates that, according to Fukui function analysis, the sulfur atoms in the carbon-sulfur groups of the three collectors exhibit the highest f_{w+} and f_{w-} values. Notably, f_{w-} surpasses f_{w+}, suggesting electron-donating characteristics, aligning with the HOMO analysis. In comparison, the acetylene group C23 in PDEC (f_{w+}=0.102) shows a greater electron-accepting ability than C24 (f_{w+}=0.065) in chelating group of Al-DECDT, facilitating nucleophilic interactions between electron-rich metal compounds and electron-deficient acetylene groups.

Table 3. Fukui function of collectors.

Collectors	Atoms	f_{w+}	f_{w-}
PDEC	S2	0.280	0.421
	C1	0.079	0.017
	N7	0.039	0.026
	S3	0.158	0.154
	C23	0.102	0.081
Z-200	S4	0.365	0.572
	C3	0.154	0.078
	N5	0.052	0.028
	O2	0.064	0.013
Al-DECDT	S2	0.266	0.414
	C1	0.068	0.019
	N7	0.040	0.026
	S3	0.138	0.161

 doi:10.20944/preprints202401.1544.v1

	C24	0.065	0.034

3.3. Adsorption Energy Comparison

In this work, the carbon-sulfur group serves as the reaction center, with the S atom strategically positioned above an Au atom. For assessed the efficacy of the acetylene group in enhancing the adsorption of collectors on the Au(111) surface, accordingly, the acetylene group bond in PDEC and the carbon-carbon double bond in Al-DECDT were aligned parallel to another Au atom. Post-optimization analysis revealed that the most efficient adsorption occurred when the carbon-sulfur double bonds were oriented flat against the crystal surface [32], with the S atom directly above the Au atom, yielding the maximum adsorption energy. Figure 4 illustrates the optimal configurations of the collectors on the Au(111) surface, as established through DFT calculations.

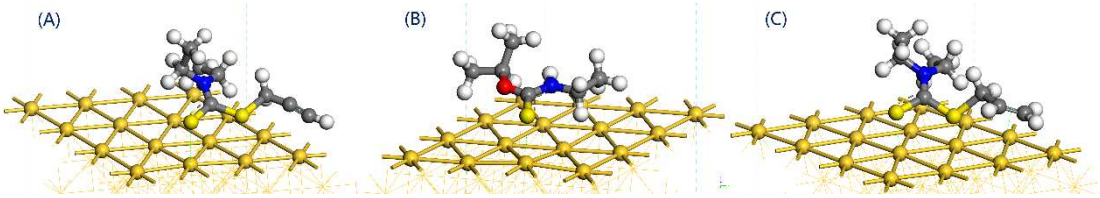

Figure 4. Adsorption configuration of (A) PDEC, (B) Z-200, (C) Al-DECDT on the Au (1 1 1) surface, (where golden yellow, yellow, gray, blue, red, white spheres represent Au, S, C, N, O, H atoms, respectively).

Table 4 delineates the adsorption energy and bond lengths of collectors on the Au(1 1 1) surface. The adsorption energy follows the sequence: PDEC> Al-DECDT> Z-200. Post-optimization, the bond lengths of the sulfur atom in the carbon-sulfur group to the Au(1 1 1) surface is Z-200< Al-DECDT< PDEC. However, it is noteworthy that in PDEC, the acetylene group is positioned significantly away from the Au(1 1 1) surface, suggesting a likelihood of weak adsorption. Consequently, these findings necessitate an in-depth analysis considering the density of states and electron density difference.

Table 4. The adsorption energy calculation and bond length of collectors on Au(1 1 1).

Collectors	Adsorption energy (KJ/ mol)	S-Au bond length (Å)
PDEC	-71.46259119	2.580
Z-200	-58.05373004	2.521
Al-DECDT	-59.43253585	2.557

3.4. Density of States Analysis

PDEC, characterized by its acetylene content, is classified as a non-ionic polar collector. Investigating the interactions between PDEC atomic orbitals and the Au(1 1 1) surface is pivotal in elucidating the chemical interactions between PDEC and gold ore surfaces. Figure 5 illustrates the density of states for the collector both pre- and post-adsorption onto the Au(1 1 1) surface. To delve into the interaction dynamics of PDEC with the Au(1 1 1) surface, a comparative study was conducted, focusing on the variations in the density of states of the S atom within the carbon-sulfur group, and the terminal hydrocarbon group of the polar moiety (specifically, the acetylene group in PDEC and the olefin group in Al-DECDT) during the adsorption process.

 doi:10.20944/preprints202401.1544.v1

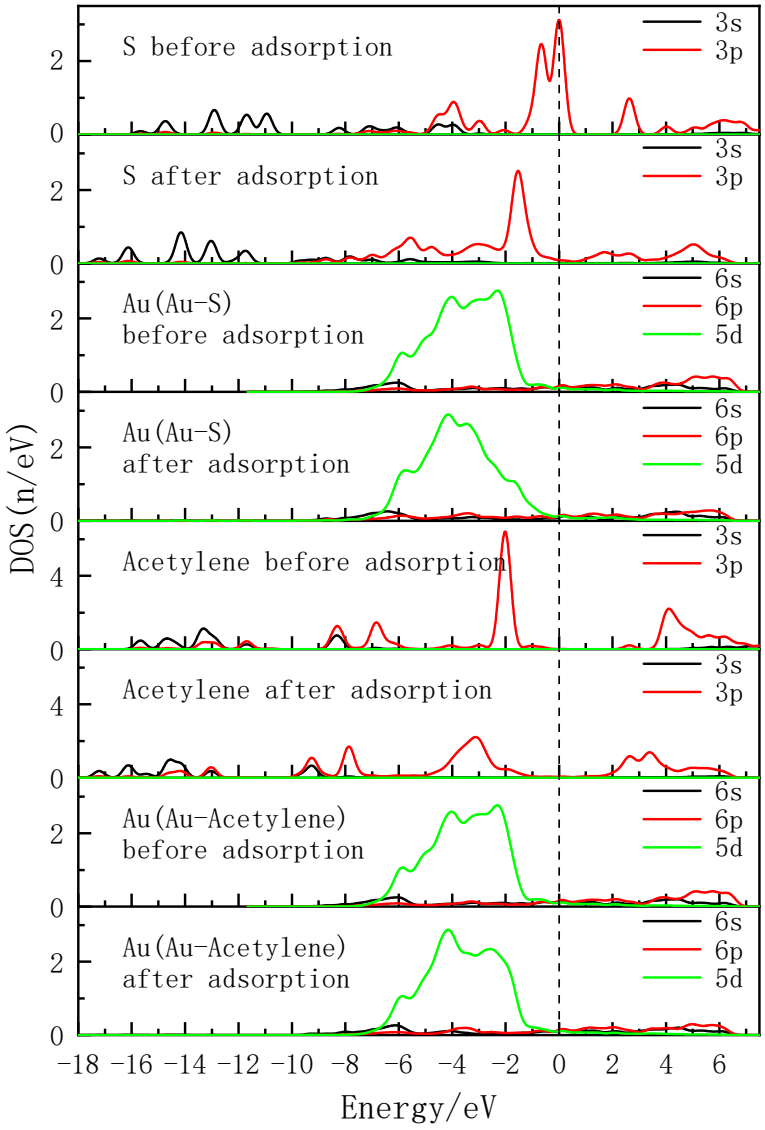

Figure 5. Density of states between PDEC on the Au(1 1 1) surface before and after interaction.

Figure 5 delineates the density of states of sulfur atoms, the acetylene group, and the corresponding gold atoms on surface of Au(1 1 1) in PDEC. At the Fermi level, the energy is normalized to zero, with the DOS spectrum spanning from -18 to 8 eV. This region primarily encompasses the bonding and antibonding states of S 3p, C 2p, and Au 5d orbits. Within PDEC, the 3p orbit of S in the carbon-sulfur double bond traverses the Fermi level. Initially, this 3p state is highly localized; however, post-adsorption, there is a notable shift in density of states of S toward lower energy levels. This shift signifies electron loss and an increase in sulfur's oxidative capacity. Concurrently, there is a reduction in the non-locality of the bonded Au atom's 5d orbit. Notably, the S 3p and Au 5d orbit hybridize at -2 to -1 eV and -8 to -7 eV, suggesting robust interactions between S and Au atoms, with sulfur donating electrons to form a positive bond with gold. Similarly, the contribution of acetylene, primarily from the C 2p orbit near the Fermi level, exhibits a marked localization at -2 eV before adsorption. Following adsorption, the density of states of acetylene group shifts toward lower energy levels, accompanied by a pronounced reduction in the density peak and increased non-locality of the C 2p orbit. This trend is also mirrored in the density of states of Au atom, which shifts modestly toward lower energies. Hybridization between the C 2p and Au 5d orbits at -2 to -1 eV and -8 to -6 eV indicates a weaker feedback bond formation between the acetylene group and the Au atom.

 doi:10.20944/preprints202401.1544.v1

3.5. Electron Density Difference

Figures 6(a) and (b) illustrate the local electron differential density of the S atom in PDEC's carbon-sulfur group and the acetylene group on the Au(1 1 1) surface. Red and blue denote electron enrichment and depletion, respectively. The contour levels depicted range from 0.2 (red) to -0.2 (blue) e/Å3, where deeper colors signify greater electron enrichment or depletion. In the carbon-sulfur group, the S atom lose electrons to the corresponding Au atom, leading to electron concentration between them, indicative of a strong interaction. Conversely, the C atom at the ends of the acetylene group lose electrons, enriching the electrons on the triple bond, while the corresponding Au atom also lose electrons and overlap with acetylene. Notably, the Au atom associated with the acetylene group lose fewer electrons than those associated with the S atom, implying a weaker interaction with the acetylene group.

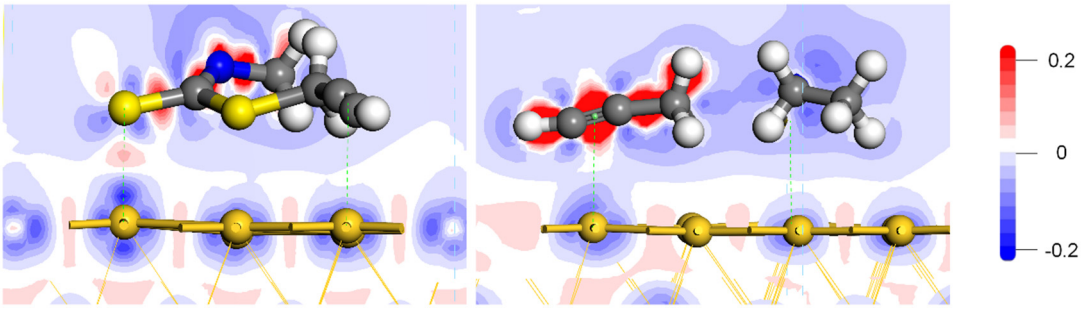

Figure 6. Electron density difference of PDEC adsorbed on the Au (1 1 1) surface, (a) electron density difference of the S atom in PDEC's carbon-sulfur group on the Au (1 1 1) surface; (b) electron differential density of PDEC's acetylene group on the Au (1 1 1) surface.

Table 5 offers a detailed atomic Mulliken charge populations, elucidating the electron transfer dynamics. Upon adsorption of PDEC onto the Au(1 1 1) surface, the Au atom linked to the S atom in the carbon-sulfur group exhibit a minor electron loss in the 6s and 5d orbits, whereas their 6p orbit gain a substantial number of electrons, supplied by the S 3p orbit. The 3p orbit of the C atom in the acetylene group receive some electrons from the corresponding Au atom, forming back-donation bond.

Table 5. Mulliken populations of PDEC atom and Au (1 1 1) atom before and after PDEC adsorbed on the Au (1 1 1) surface.

Atomic label	Adsorption status	s	p	d	Charge/e
S	Before adsorption	1.83	4.31	0.00	-0.14
	After adsorption	1.83	4.17	0.00	0.00
Au(Au-S)	Before adsorption	0.91	0.53	9.65	-0.09
	After adsorption	0.85	0.72	9.62	-0.18
C	Before adsorption	1.15	3.23	0.00	-0.38
	After adsorption	1.17	3.19	0.00	-0.36
Au(Au-C)	Before adsorption	0.91	0.53	9.65	-0.09
	After adsorption	0.83	0.46	9.63	0.08

The findings from the electron differential density and Mulliken charge populations align with the state density analysis. The S atom in PDEC's carbon-sulfur group donate electrons to the Au atom, creating strong positive coordination bond. Meanwhile, the acetylene group receives some electrons from the Au atom, resulting in comparatively weaker back-donation bond, with the positive coordination bonds being predominant.

 doi:10.20944/preprints202401.1544.v1

3.6. Adsorption Experiments

Samples of 50ml each of PDEC, Z-200, and Al-DECDT solutions at various concentrations were prepared. Following the interaction between these collector solutions and the gold powder, their absorbance was measured at their respective maximum absorption wavelengths—252nm, 246nm, and 258nm—using a UV-Visible Spectrophotometer. This procedure aimed to determine the quantity of each collector adsorbed onto the gold powder's surface. Figure 7 illustrates the correlation between the adsorption amount and the initial concentration of the collectors. It was noted that the adsorption amount on the gold powder surface proportionally increased with the initial concentration of the collectors. The sequence of adsorption efficiency on the gold powder surface was observed as PDEC > Al-DECDT > Z-200, suggesting that PDEC possesses the most potent collecting capability for gold powder.

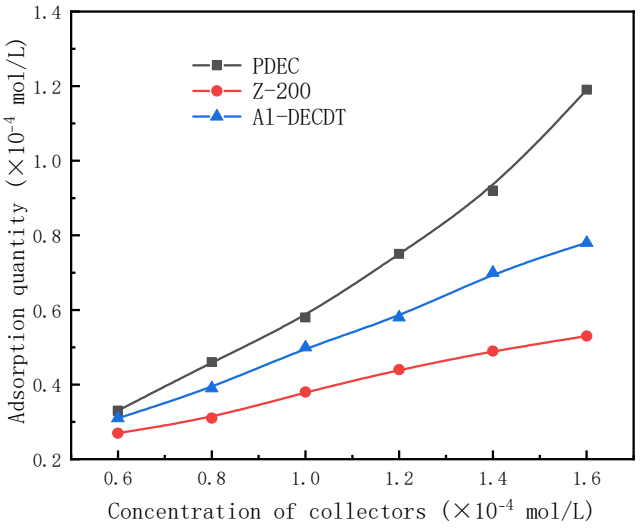

Figure 7. Adsorption quantity of PDEC, Z-200, and Al-DECDT on gold powder surfaces as a function of concentration.

4. Conclusions

(1) In PDEC, the carbon-sulfur group form covalent bonds characterized by shorter bond lengths, the reduced carbon-sulfur double bonds and lower Mulliken population of S atom lead to enhanced electron localization. This attribute grants PDEC superior selectivity during its adsorption on mineral surfaces.

(2) Analysis of the LUMO+1 orbit indicates that the electrons in acetylene group of PDEC are delocalized, significantly contributing to the molecule's frontier orbital energy. The C atom in this group (fw+=0.102) demonstrate a robust electron-accepting capacity, underscoring the crucial role of acetylene group in facilitating bonding interactions with mineral surfaces, particularly in accepting electrons from mineral metal atoms to form stable back-donation bonds.

(3) Both the S atom in the carbon-sulfur group and the acetylene group of PDEC establish stable adsorption structures with the Au(1 1 1) surface, adopting a single coordination mode. The adsorption energy as follows: PDEC > Al-DECDT > Z-200. Partial density of states analysis shows that PDEC's S 3p orbit hybridize with Au 5d orbit, forming robust coordination bonds. Conversely, the C 2p orbit in the acetylene group engage in weaker back-donation bonding with Au 5d orbit. This is further corroborated by the electron density difference and post-adsorption Mulliken population, which confirm the electron donation by PDEC's S atom to the Au atom, while the acetylene group predominantly accepts electrons, with positive coordination bonds being the primary interaction in the adsorption process.

(4) In adsorption experiments, the adsorption quantity of collectors adsorbed onto gold powder surfaces was quantified using a UV-Visible Spectrophotometer. The adsorption quantity was

 doi:10.20944/preprints202401.1544.v1

observed to increase proportionally with the initial concentration, following the order: PDEC > Al-DECDT > Z-200. These experimental outcomes align with the DFT adsorption energy results.

References

1. Wu, J.; Ahn, J.; & Lee, J. Gold deportment and leaching study from a pressure oxidation residue of chalcopyrite concentrate. Hydrometallurgy.2021,201, 105583.
2. Yang, H. Y.; Wang, S. H.;Song, X. L., & Pan, H. D. Gold occurrence of Jiaojia gold mine in Shandong province. Transactions of Nonferrous Metals Society of China. 2011,21(9), 2072-2077.
3. Arif, J.; & Baker, T. Gold paragenesis and chemistry at Batu Hijau, Indoneisa: implications for gold-rich porphyry copper deposits. Mineralium Deposita. 2004 39, 523-535.
4. Asamoah, R. K. Specific refractory gold flotation and bio-oxidation products: Research overview. Minerals. 2021, 11(1), 93.
5. Tagirov, B. R.; Filimonova, O. N.;Trigub, A. L.; Vikentyev, I. V.; Kovalchuk, E. V.; Nickolsky, M. S.; Chareev, D. A. The state of gold in phases of the Cu-Fe-S system: In situ X-ray absorption spectroscopy study. Geoscience Frontiers. 2023, 14(3), 101533.
6. El-Sayed, S.; El-Shatoury, E. H.; Abdel-Khalek, N. A.; Abdel-Motelib, A.; Abdel-Khalek, M. A. Influence of Bacillus cereus-gold interaction on bio-flotation of gold in the presence of potassium butyl xanthate. Biointerface Research in Applied Chemistry. 2021, 11(5), 13005-18.
7. Wang, S.; Zhang, L.; Lu, D.; Fu, Y. Identification of abnormal conditions for gold flotation process based on multivariate information fusion and double-channel convolutional neural network. The Canadian Journal of Chemical Engineering. 2023.
8. Akop, C. Developing a bulk circuit suitable for chalcopyrite-pyrite ores with elevated pyrite content in copper-gold ore treatment. 2014.
9. Bas, A. D.; Larachi, F. The effect of flotation collectors on the electrochemical dissolution of gold during cyanidation. Minerals Engineering. 2019,130, 48-56.
10. Matveeva, T. N.; Gromova, N. K.; Lantsova, L. B. Experimental Proof of Applicability of Cyclic and Aliphatic Dithiocarbamate Collectors in Gold-Bearing Sulphide Recovery from Complex Ore. Journal of Mining Science. 2021, 57, 123-130.
11. Liu, G.; Yang, X.; Zhong, H. Molecular design of flotation collectors: A recent progress. Advances in Colloid and Interface Science. 2017, 246, 181-195.
12. Oluwabunmi, K. E.; Adeleke, A. A.; Adetunji, A. R.; Jeje, S. O.; Abioye, A. A.; Adesina, O. A.; Ibitoye, F. P. 2 k Factorial Experiments on Factors that Influence the Recovery of Gold during the Upgrade of Ilesha-Itagunmodi Gold Ore through Froth Flotation. Journal of Minerals and Materials Characterization and Engineering, 2014.
13. Tan, L., Lin, Q., Liu, P., & Fu, L. Studies on the flotation separation of a new thionocarbamate--ZL 4020. Mining and Metallurgical Engineering(China)(China), 1996, 16(3), 26-29.
14. Beattie, D. A., Kempson, I. M., Fan, L. J., & Skinner, W. M. Synchrotron XPS studies of collector adsorption and co-adsorption on gold and gold: silver alloy surfaces. International Journal of Mineral Processing , 2009, 92(3-4), 162-168.
15. Ha, C. S.; Nagappan, S. Hydrophobic and Superhydrophobic Organic-Inorganic Nano-Hybrids. CRC Press. 2018.
16. Nosáľová, L.; Maliničová, L.; Kisková, J.; Timková, I.; Sedláková-Kaduková, J.; Pristaš, P. Cultivable microbiota associated with gold ore from the rozália gold mine, hodruša-hámre, Slovakia. Geomicrobiology Journal. 2021 38(5), 415-425.
17. Burdonov, A.; Vchislo, N.; Barakhtenko, V.; & Sahabutdinova, T. Synthesized collectors flotation activity study based on fluorine containing and acetylene alcohols. Sustainable Development of Mountain Territories. 2023, 15(3), 707-719.
18. Yushina, T. I. Justification of applying collectors from the class of unsaturated tertiary alcohols in flotation of gold-bearing sulphide ores.2022.
19. Liu, W.; Miller, J. D.; Sun, W.; Hu, Y. Analysis of the selective flotation of elemental gold from pyrite using diisobutyl monothiophosphate. Minerals. 2022, 12(10), 1310.
20. Dong, Z.; Jiang, T.; Xu, B.; Zhong, H.; Zhang, B.; Liu, G.;Yang, Y. Density functional theory study on electronic structure of tetrahedrite and effect of natural impurities on its flotation property. Minerals Engineering. 2021, 169, 106980.

21. Mkhonto, P. P.; Chauke, H. R.; Ngoepe, P. E. The effect of thiol collectors on nickel-rich (110) pentlandite surface using density functional theory. Proceedings of SAIP2017. 2018, 95-100.
22. Yuan, M.; Feng, X.; Yan, T. H.; Chen, J.; Ma, X.; Cunha, P.; Wang, Y. Superparamagnetic iron oxide-enclosed hollow gold nanostructure with tunable surface plasmon resonances to promote near-infrared photothermal conversion. Advanced Composites and Hybrid Materials. 2022, 5(3), 2387-2398.
23. Nenchev, G.; Diaconescu, B.; Hagelberg, F.; Pohl, K. Self-assembly of methanethiol on the reconstructed Au (111) surface. Physical Review B. 2009, 80(8), 081401.
24. He, J.; Sun, W.; Chen, D.; Gao, Z.; Zhang, C. Interface interaction of benzohydroxamic acid with lead ions on oxide mineral surfaces: a coordination mechanism study. Langmuir. 2021, 37(11), 3490-3499.
25. He, Y.; Wang, Z.; Ren, Z.; Zheng, R.; Gao, H.; Chen, Z. The Influence of Surface Heterogeneity of Fluorite on the Adsorption of Alkyl Sulfonates. Minerals. 2023, 13(8), 1005.
26. Xu, B.; Wu, J.; Dong, Z.; Tao, J.; Qian, L.; Yang, Y. Flotation performance, structure–activity relationship and adsorption mechanism of a newly-synthesized collector for copper sulfide minerals in Gacun polymetallic ore. Appl. Surf. Sci. 2021, 551, 149420.
27. Cao, S.; Cao, Y.; Liao, Y.; Ma, Z. Depression mechanism of strontium ions in bastnaesite flotation with salicylhydroxamic acid as collector. Minerals 2018, 8, 66.
28. Corso, M.; Fernández, L.; Schiller, F.; Ortega, J. E. Au (111)-based nanotemplates by Gd alloying. ACS nano. 2010, 4(3), 1603-1611.
29. Li, M.; Sun, B.; Ao, Z.; An, T.; Wang, G. Atomic-scale identification of influencing factors of sodium dendrite growth on different current collectors. J. Mater. Chem. A 2020, 8, 10199–10205.
30. Mishra, S.; Panda, S.; Akcil, A.; Dembele, S. Biotechnological avenues in mineral processing: Fundamentals, applications and advances in bioleaching and bio-beneficiation. Mineral Processing and Extractive Metallurgy Review. 2023, 44(1), 22-51.
31. Terzi, M.; Kursun, I.; Cinar, M.; Ozdemir, O. Digital image processing (DIP) application on the evaluation of ironrich heavy mineral concentrates produced from river sand using a sequential mineral processing approach. Physicochemical Problems of Mineral Processing. 2021, 57.
32. Yang, K.; Lu, X. C.; Liu, X. D.; Hou, Q. F. Characterization technique ⅱ of mineral material based on probe gas adsorption isotherm: nano-pore structure of porous material. Bulletin of mineralogy petrology and geochemistry. 2006, 25(4), 362-368.
33. Tkatchenko, A.; Scheffler, M. Accurate Molecular Van Der Waals Interactions from Ground-State Electron Density and Free-Atom Reference Data. J. Phys. Rev. Lett. 2009, 102, 073005.
34. Zierhut, A., Leopold, K., Harwardt, L., Worsfold, P., & Schuster, M. Activated gold surfaces for the direct preconcentration of mercury species from natural waters. Journal of Analytical Atomic Spectrometry, 2009, 24(6), 767-774.